Mo + C Codoped TiO_2 Using Thermal Oxidation for Enhancing Photocatalytic Activity

Jun Zhang,[†] Chunxu Pan,[*,†,‡] Pengfei Fang,[†] Jianhong Wei,[†] and Rui Xiong[†]

Key Laboratory of Artificial Micro- and Nano-structures of Ministry of Education and School of Physics and Technology and Center for Electron Microscopy, Wuhan University, Wuhan 430072, P.R. China

ABSTRACT The photocatalytic activity of TiO_2 is enhanced mainly through heightening absorption of UV−vis light and improving the separation efficiency of photoinduced electrons and holes. The recent new theoretical research revealed that the TiO_2 codoped with Mo + C is considered to be an optimal doping system. On the basis of this theory, the Mo + C codoped TiO_2 powders were first experimentally synthesized by thermal oxidizing a mixture of TiC and MoO_3 powders in the air. The XRD patterns and the XPS survey spectrum showed that carbon (C) acted as a Ti−O−C band structure and molybdenum (Mo) existed as Mo^{6+} in anatase TiO_2. The Mo+C codoped TiO_2 had a 32 nm red shift of the spectrum onset compared with pure anatase TiO_2, and its band gap was reduced from 3.20 to 2.97 eV. The photocurrent of the Mo + C codoped TiO_2 was about 4 times as high as that of pure anatase TiO_2, and its photocatalytic activity on decomposition of methylene blue was enhanced.

KEYWORDS: titanium dioxide • photocatalysis • Mo + C codoping • thermal oxidation

1. INTRODUCTION

It is well-known that TiO_2 is an excellent and highly efficient photocatalyst. However, the large band gap of 3.20 eV makes it absorb only ultraviolet light with a wavelength of no longer than 387 nm, which leads to a low utilization ratio of solar light. Generally, there are several methods for enhancing the photocatalytic activity of TiO_2, such as nonmetal doping, metal doping, semiconductor compounding, and dye sensitization. In non-metal-doped TiO_2, some of the lattice oxygen atoms will be substituted to reduce the band gap. This non-metal-doped TiO_2 shows a red shift of the spectrum onset and a higher absorption for the visible light. The transition metal doped TiO_2 will form a deep energy level so that electrons and holes can be excited by low energy photons, which also increases the absorption of the visible light.

Up to now, various nonmetal and metal elements, such as N (1, 2), S (3, 4), C (5–12), Fe (13), and Mo (14), have been successfully doped into TiO_2 nanomaterials. Irie H et al. (10) fabricated the C-doped TiO_2 powders by oxidative annealing of TiC at low-temperature 350 °C in the air, and they found that the C-doping caused the absorbance edge of TiO_2 to a higher wavelength region. Shen M et al. (12) showed that the C-doped TiO_2 obtained by oxidative annealing of TiC had much higher photocatalytic activity compared with pure anatase TiO_2 under the visible light.

However, many studies have demonstrated that the monodoping will generate recombination centers inside the TiO_2, which goes against the light-induced charge carriers' migration to the surface for photocatalyzing (15, 16). It has been recognized that the codoped TiO_2 with both nonmetal anions and metal cations can reduce the recombination centers because of the neutralization of positive and negative charges inside TiO_2, which can effectively improve the charge carriers' migration efficiency and then enhance the photocatalytic activity (17).

Recently, Gai Y et al.'s (16) theoretical calculations revealed that the Mo + C codoped TiO_2 had the following advantages: (1) the C doping can shift the valence band edge effectively to heighten absorption for the visible light; (2) in the case of the conduction band edge being almost unchanged, the higher reducing potential and the stronger reducing power remain, guaranteeing the good photodegradaton property of the TiO_2; (3) this codoped system can also decrease the formation of the recombination centers inside the TiO_2 and increase the migration efficiency of the light-induced charge carriers. They concluded that this Mo + C codoped TiO_2 provided a possible optimal doping system. According to the theory results in the ref 16, the present work tries to experimentally fabricate the Mo + C codoped TiO_2 material by using a thermal oxidation process and to evaluate its photocatalytic properties.

2. EXPERIMENTAL SECTION

Synthesis of the C-Doped TiO_2. TiC powders were bestrewed on a quartz plate and mildly oxidized in the air at 350 °C for 20 h and then annealed at 600 °C for 10 min. The resulting sample was a kind of yellowish powders.

Synthesis of the Mo+C Codoped TiO_2. TiC and MoO_3 powers were mixed in a molar ratio of 100:1 and then ball-milled for

* Corresponding author. Tel.: +86-27-6875-2969. Fax: +86-27-6875-2003. E-mail: cxpan@whu.edu.cn.

Received for review January 6, 2010 and accepted March 1, 2010

† Key Laboratory of Artificial Micro- and Nano-structures of Ministry of Education and School of Physics and Technology, Wuhan University.

‡ Center for Electron Microscopy, Wuhan University.

DOI: 10.1021/am100011c

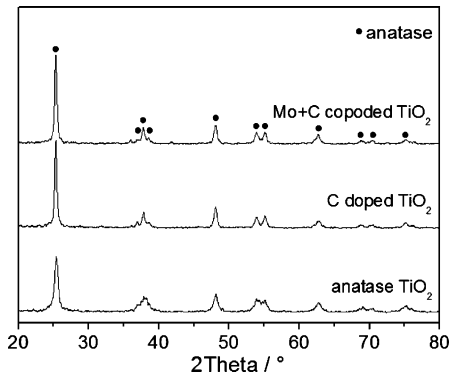

FIGURE 1. XRD patterns of Mo + C codoped TiO_2, C-doped TiO_2, and anatase TiO_2.

4 h for sufficient mixing. The thermal oxidization process was the same as above.

For comparison, the commercial pure anatase TiO_2 powers were purchased from the Hefei Kejing Materials Technology Co., LTD, CHINA.

Characterizations. The crystal phases of the photocatalysts were measured using an X-ray diffractometer (XRD) (D8 Advanced XRD, Bruker AXS, Germany) with Cu K alpha radiation. X-ray photoelectron spectroscopy (XPS) measurements were performed in a VG Multilab2000 spectrometer to have the information on chemical binding energy of the photocatalysts. UV−vis diffuse reflectance spectra (DRS) of the photocatalysts and the visible absorption spectra of methylene blue in the photocatalytic experiment were measured by using a UV−vis spectrophotometer (UV-2550, Shimadzu, Japan).

Photocurrent Tests. Briefly, 5 mg of photocatalyst was dispersed in 5 mL of ethanol and ultrasonically vibrated for 30 min. The 0.25 mL resultant slurry was then dip-coated onto a 10 × 20 mm indium−tin oxide (ITO) glass electrode and dried under high-pressure mercury lamp irradiation to eliminate ethanol. The prepared TiO_2/ITO electrode, platinum electrode, and saturation calomel electrode (SCE) were used as the working electrode, counter electrode, and reference electrode, respectively. The electrolyte was the 0.5 mol/L Na_2SO_4 aqueous solution. The working electrode was activated in the electrolyte for 2 h before measurement. A high-pressure mercury lamp (160 W) was used as a light source away from the working electrode with a distance of 15 cm. All the experiments were conducted at room temperature.

Photocatalytic Experiments. The photocatalytic activity of the photocatalysts was measured by the decomposition of methylene blue. A 250 W high-pressure mercury lamp which generates light in the 350−450 nm range with a maximum intensity at 365 nm was used as a light source. The lamp was in a distance of 25 cm above the liquid surface. The 100 mg photocatalysts were put into 100 mL of a 12 mg/L methylene blue solution. The mixed solution was stirred incessantly, and after every 90 min, 3 mL solution was took out to test the residual concentration of methylene blue, which was evaluated by measuring the change of maximum absorbance in the UV−vis spectrometry.

3. RESULTS AND DISCUSSION

Figure 1 illustrates the XRD patterns for pure anatase, C-doped, and Mo + C codoped TiO_2. Obviously, only an anatase phase can be observed in all samples. That is to say, no TiC and MoO_3 peaks are detected from the XRD pattern of Mo + C codoped TiO_2, which indicates that the TiC powers were oxidized completely and the Mo ion was doped into the anatase TiO_2.

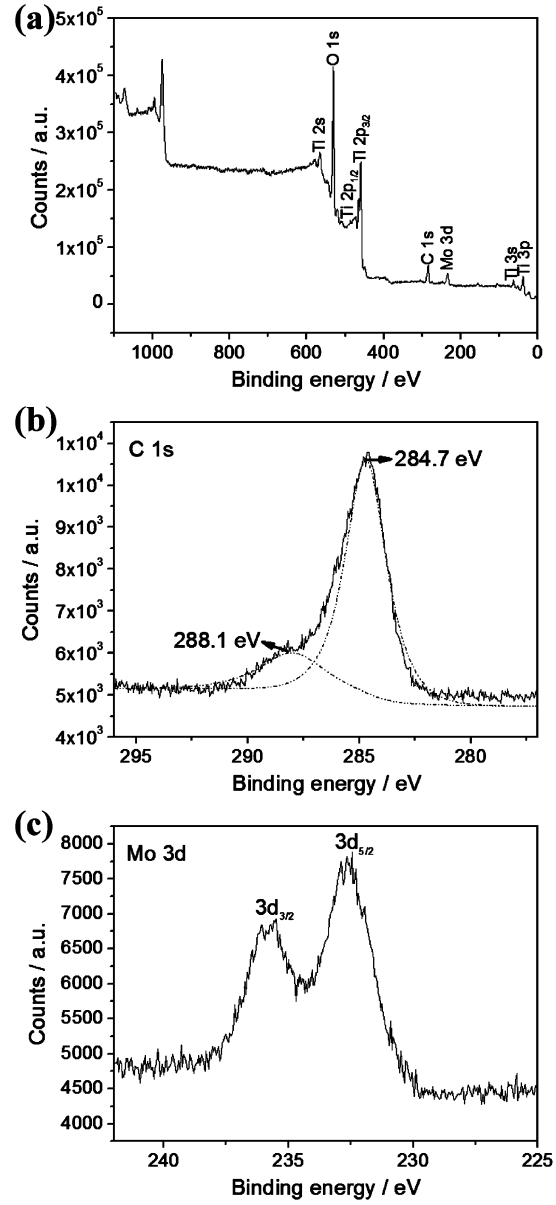

FIGURE 2. XPS spectra of (a) survey spectrum, (b) C 1s, and (c) Mo 3d for Mo + C codoped TiO_2.

The XPS survey spectrum of the Mo + C codoped TiO_2 reveals that the powders contain four elements Ti, O, C, and Mo, in which the chemical binding energies for Ti $2p_{3/2}$, O 1s, C 1s, and Mo 3d are 458.6, 532.0, 284.7, and 232.5 eV respectively, as shown in Figure 2a. To investigate the carbon states in the sample, the C 1s core levels were measured, as shown in Figure 2b. It was found that there were two peaks at the binding energies of 284.7 and 288.1 eV. Generally, the peak at 284.7 eV is a signal of adventitious elemental carbon as in other works (8, 10), and the peak at 288.1 eV demonstrates the presence of the C−O bonds. The atom content of doped C was estimated to be 2.56% by comparing the product of the 288.1 eV peak area multiplied by the C element sensitive factor to the product of all peaks multiplied by respective element sensitive factor. This reveals that the C atoms substitute parts of the Ti lattice-point and form a Ti−O−C band structure. In addition, the examination on the Mo 3d core levels confirms the element Mo

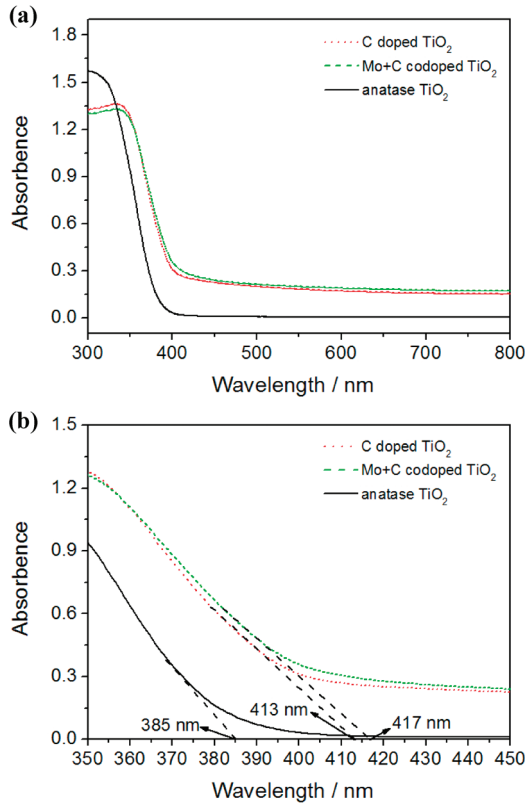

FIGURE 3. UV−vis diffuse reflectance spectra of (a) survey spectrum, (b) local spectrum for Mo + C codoped TiO_2, C-doped TiO_2, and anatase TiO_2.

exists as a Mo^{6+} which is similar with other work (18), as shown in Figure 2c. The atom content of doped Mo was estimated to be 1.66% by the some calculating method. Combined with the XRD results without MoO_3 phase, it can be inferred that the element Mo has been doped into anatase TiO_2 lattice as a Mo^{6+}.

Figure 3 illustrates the UV−vis DRS of pure anatase, C-doped, and Mo + C codoped TiO_2. The survey spectra of the C-doped and Mo + C codoped TiO_2 exhibit similar variations. However, comparing with the pure anatase TiO_2, they have a red shift of the spectrum onset and a stronger absorption in the visible light range, as shown in Figure 3a. The local spectra (Figure 3b) indicate that the onset of the absorption spectrum of pure anatase TiO_2 appears at 385 nm and the spectrum onset of the C-doped TiO_2 appears at 413 nm. Obviously, the onset of the C-doped TiO_2 shows a 28 nm red shift comparing with pure anatase TiO_2. According to the equation $\lambda = 1240/E_g$, the band gap of the C-doped TiO_2 is 3.0 eV, which is similar to other research (10–12). However, this band gap seems much higher than Gai et al.'s calculated value of 2.27 eV (16).

The reasons for this deviation may be as follows: (1) the actual experimental C-doping content is perhaps much lower than that in the theoretical model, and practically, the C-doping content in TiO_2 can not be controlled during thermal oxidation of TiC; (2) influence of the absorption, such as N_2 molecule, on the surface of the C-doped TiO_2, which generally results in a great effect on the experimental data, whereas the absorption was not considered in the

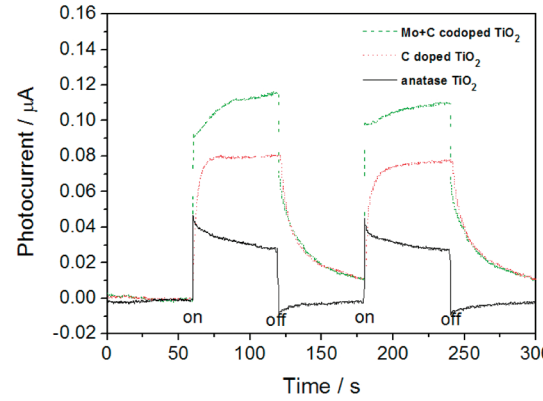

FIGURE 4. Photoelectrochemical responses of Mo + C codoped TiO_2, C-doped TiO_2, and anatase TiO_2.

theoretical calculation (16). Additional Mo doping makes only a small change in the onset of the absorption spectrum (417 nm); there is a little more red shift (4 nm), and the band gap is reduced (2.97 eV).

Gai et al.'s Mo + C codoping calculation results indicated that the purpose of C doping in TiO_2 was to shift up the valence band edge and reduce the band gap, and the Mo doping was to avoid generating carrier recombination centers due to the C doping, whereas there was no affect upon variation on the conduction band edge and thus retaining the reducing power of TiO_2 (16). The present experiments demonstrate that the influence of Mo + C codoping on the energy band TiO_2 is coincident to the Gai et al.'s calculation (16); however, only the band gap is not as narrow as the calculation. Further work is being focused upon the process for increasing C content during Mo + C codoping.

For the effect of Mo + C codoping upon the separation efficiency of photoinduced electrons and holes in TiO_2, it has been recognized that the C doping generally tends to form recombination centers inside the TiO_2 and inhibits the charge carriers migrate to the surface for photocatalyzing, whereas the Mo + C codoping could effectively avoid the generation of the carrier recombination centers (16).

Figure 4 gives the photoelectricity of the TiO_2 samples by using a photocurrent test. The potential of the working electrode against a Pt counter electrode was set at 0.0 V. A uniform photocurrent response was observed for each switch-on and switch-off event in all electrodes. When the cutoff filter was absent, it was found that the photocurrent of the pure anatase, C-doped, and Mo + C codoped TiO_2 electrodes were 0.03, 0.08, and 0.12 μA, respectively. The photocurrent of the C-doped TiO_2 electrode was about three times as high as that of the pure anatase TiO_2 electrode; because C doping led to a red shift of the spectrum onset and higher absorption in the visible light in the 380−800 nm range. And the Mo + C codoped TiO_2 sample increased the photocurrent further to be four times as high as that of the pure anatase TiO_2 electrode. The photocurrent was in the order of Mo + C codoped TiO_2 > C-doped TiO_2 > pure anatase TiO_2. Compared with the C-doped TiO_2, the Mo + C codoped TiO_2 has a similar absorption in UV−vis light, but can generate much more photoinduced electrons and holes because of the higher photocurrent. These experimental

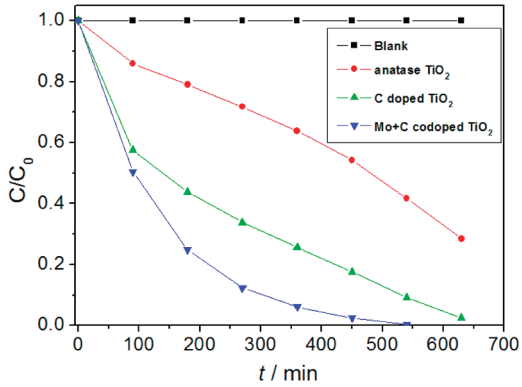

FIGURE 5. Methylene blue decomposition upon irradiation.

results demonstrate that the Mo + C codoped TiO_2 really decreases the carrier recombination centers and improves the separation efficiency of photoinduced electrons and holes in TiO_2, which is coincident to Gai et al.'s conclusions (16).

Figure 5 shows the decompositions of methylene blue. The photocatalytic activity is in the order of the Mo + C codoped TiO_2 > C-doped TiO_2 > pure anatase TiO_2, which is also consistent with the photocurrent experiments, as shown in Figure 4. These results further demonstrate that the Mo + C codoped TiO_2 possess a higher photocatalytic activity because of the decrease in carrier recombination centers and increase in the separation efficiency of the photoinduced carrier.

4. CONCLUSIONS AND SUMMARIES

Mo + C codoped TiO_2 powers were obtained by thermal oxidation the mixture of TiC and MoO_3 in the air. This Mo + C codoped TiO_2 can absorb visible light, have higher separation efficiency of photoinduced electrons and holes, and possess higher photocatalytic activity compared with anatase TiO_2. But the band gap of Mo + C codoped TiO_2 was not as narrow as the simulation and calculation because of some differences between the practical sample and simulation model such as lower doping content of C and N_2 molecule that may be absorbed on the surface of TiO_2. Other doping methods will be considered to increase the doping content of C.

Acknowledgment. This work was supported by the Specialized Research Fund for the Doctoral Program of Higher Education (20070486016), Ministry of Education, China, National Basic Research Program of China (973 Program) (2009CB939700), and PhD candidates self-research (including 1 + 4) program of Wuhan University in 2008 (20082020201000004).

REFERENCES AND NOTES

(1) Asahi, R.; Morikawa, T.; Ohwaki, T.; Aoki, K.; Taga, Y. *Science* **2001**, *293*, 269–271.
(2) Ihara, T.; Miyoshi, M.; Iriyama, Y.; Matsumoto, O.; Sugihara, S. *Appl. Catal., B* **2003**, *42*, 403–409.
(3) Umebayashi, T.; Yamaki, T.; Itoh, H.; Asai, K. *Appl. Phys. Lett.* **2002**, *81*, 454–456.
(4) Ohnoa, T.; Akiyoshi, M.; Umebayashi, T.; Asai, K.; Mitsui, T.; Matsumura, M. *Appl. Catal., A* **2004**, *265*, 115–121.
(5) Shahed, U. M.; Mofareh, A. S.; William, B. I. *Science* **2002**, *297*, 2243–2245.
(6) Janus, M.; Tryba, B.; Inagaki, M.; Morawski, A. W. *Appl. Catal., B* **2004**, *52*, 61–67.
(7) Wang, X.; Meng, S.; Zhang, X.; Wang, H.; Zhong, W.; Du, Q. *Chem. Phys. Lett.* **2007**, *444*, 292–296.
(8) Ren, W.; Ai, Z.; Jia, F.; Zhang, L.; Fan, X.; Zou, Z. *Appl. Catal., B* **2007**, *69*, 138–144.
(9) Kang, I. C.; Zhang, Q.; Yin, S.; Sato, T.; Saito, F. *Appl. Catal., B* **2008**, *80*, 81–87.
(10) Irie, H.; Watanabe, Y.; Hashimoto, K. *Chem. Lett.* **2003**, *32*, 772–773.
(11) Choi, Y.; Umebayashi, T.; Yoshikawa, M. *J. Mater. Sci.* **2004**, *39*, 1837–1839.
(12) Shen, M.; Wu, Z.; Huang, H.; Du, Y.; Zou, Z.; Yang, P. *Mater. Lett.* **2006**, *60*, 693–697.
(13) Yu, J.; Xiang, Q.; Zhou, M. *Appl. Catal., B* **2009**, *90*, 595–602.
(14) Devi, G. L.; Kumar, G. S.; Murthy, N. B.; Kottam, N. *Catal. Commun.* **2009**, *10*, 794–798.
(15) Umebayashi, T.; Yamaki, T.; Itoh, H.; Asai, K. *J. Phys. Chem. Solids* **2002**, *63*, 1909–1920.
(16) Gai, Y.; Li, J.; Li, S. S.; Xia, J. B.; Wei, S. H. *Phys. Rev. Lett.* **2009**, *102*, 036402.
(17) Teruhisa, O.; Zenta, M.; Kazumoto, N.; Hidekazu, K.; Feng, X. *Appl. Catal., A* **2006**, *302*, 62–68.
(18) Yan, J.; Zhang, Yue.; Huang, W.; Tu, M. *Thin Solid Films* **2008**, *516*, 8554–8558.

AM100011C